Noname manuscript No.
(will be inserted by the editor)

Asymptotic-preserving numerical scheme for the electronic M_1 model in the diffusive limit.

S. Guisset · S. Brull · B. Dubroca · R. Turpault.

Received: date / Accepted: date

Abstract This work is devoted to the derivation of an asymptotic-preserving scheme for the electronic M_1 model in the diffusive regime. A numerical scheme is proposed in order to deal with the mixed derivatives which arise in the diffusive limit leading to an anisotropic diffusion. The derived numerical scheme preserves the realisibility domain and enjoys asymptotic-preserving properties correctly handling the diffusive limit recovering the relevant limit equation. In addition, the cases of non constants electric field and collisional parameter are naturally taken into account with the present approach. Numerical test cases validate the considered scheme in the non-collisional and diffusive limits.

Keywords Electronic M_1 moment model · approximate Riemann solvers · Godunov type schemes · asymptotic preserving schemes · diffusive limit · plasma physics · anisotropic diffusion.

1 Introduction

In order to initiate nuclear fusion reactions, it was proposed to use laser pulses in order to ignite a deuterium-tritium target. During this process the energy is transported from the critical surface to denser parts through the electron transport. This transport plays a key role in the understanding of plasma physical phenomena such as, parametric [46,26] and hydrodynamic [53,59,

S. Guisset
Laboratoire de Mathématiques de Versailles, bâtiment Fermat 45 avenue des États-Unis 78035 Versailles.
E-mail: sebastien.guisset@uvsq.fr

B. Dubroca
Laboratoire CELIA, Université de Bordeaux, 351 cours de la liberation, 33400 Talence.

S. Brull · R. Turpault
Institut de Mathématiques de Bordeaux, 351 cours de la liberation, 33400 Talence.

20] instabilities, laser-plasma absorption [51,34], wave damping [39,18], energy redistribution and hot spot formation [10,44]. Spitzer and Hrm were the first to proposed a electron transport theory in a fully ionised plasma without magnetic field. They derived the electron plasma transport coefficients by solving the electron kinetic equation by using the expansion of the electron mean free path over the temperature scale length (denoted ε in this paper). The results of Spitzer and Hrm have been reproduced in other works [9,3,54] using the early works of Chapman [15,16] and Enskog [25] for neutral gases. However in the case of non-local regimes [49], the Spitzer-Hrm theory is no more valid. Indeed the electron transport plasma coefficients were derived in the case where the isotropic part of the electron distribution function remains close to the Maxwellian. For example, in the context of inertial confinement fusion, the plasma particles may have an energy distribution far from the thermodynamic equilibrium so that the fluid description is not adapted. Moreover kinetic effects like the non local transport [10,44], wave damping or the development of instabilities [20] can be important over time scales shorter than the collisional time so that fluid simulations are insufficient and kinetic codes have to be considered to capture the physical processes. Therefore, a kinetic description seems unavoidable for the study of inertial confinement fusion processes. However such a kinetic description is accurate but also computationally expensive for describing most of real physical applications. Kinetic codes are often limited to time and length much shorter than those studied with fluid simulations. It is therefore an essential issue to describe kinetic effects by using reduced kinetic codes operating on fluid time scales.

Angular moments models can be seen as a compromise between kinetic and fluid models. On one hand, they have the advantage to be less computationally expensive than kinetic description since less variables are involved in the models and on the other hand they provide results with a higher accuracy than fluid models. Grad [29], initially proposed a moment closure hierarchy which leads to hyperbolic set of equations for close equilibrium flows. The hierarchy proposed is based a polynomial series expansion of a distribution function close to the Maxwellian equilibrium. However, the truncation of this expansion leads to a loose of the positivity of the distribution function and to unrealisable moments. In [41,47,48,56,1], closures based on entropy minimisation principles are investigated. It has been shown that this closure choice enables to recover fundamental properties such as the positivity of the underlying distribution function, the hyperbolicity of the model and an entropy dissipation property [30,45,41]. In this work, the moment model is based on an angular moments extraction. The kinetic equation is only integrated with respect to the velocity direction while the velocity modulus is kept as a variable. The closure used is based on an entropy minimisation principle and gives the angular M_1 model. This model is used in numerous applications such as radiative transfer [5,22, 57,17,50] or electron transport [42,21,32]. It satisfies fundamental properties and recovers the asymptotic diffusion equation in the long time and small mean free path regimes [23]. In order to perform numerical simulations, the HLL scheme [35] is often used for the M_1 electronic model because it ensures

the positivity of the first angular moment and the flux limitation property. However, this scheme does not degenerate accordingly in the diffusive limit as most of the schemes. Even if the scheme is consistent and one could use a very refined mesh with space step smaller than the mean free path, such a solution would be far too computationally expensive to be used in practice. Overcoming this major drawback a class of numerical schemes has emerged over the years called asymptotic-preserving schemes (AP). Asymptotic-preserving schemes in the sense of Jin-Levermore [37,36] are designed to handle multiscale situations and behave correctly in the asymptotic limit considered. In this context many works have been performed following different approaches in a one dimensional framework [8,2,27,40,52,19,38]. In particular, one of the most productive approach from the work of Gosse-Toscani [28] and which has been largely extended [12,11,5,14,7], is based on the modification of approximate Riemann solvers. Some works also deal with the two dimensional case [13,6]. In the present paper, the difference and the main difficulty comes from the mixed derivatives arising in the diffusive limit. In the present paper, we consider the M_1 model for the electronic transport [21,42,43,34,33]. Ions are supposed fixed and electron-electron collisions are not considered. The angular moment model studied reads

$$\begin{cases} \partial_t f_0(t,x,\zeta) + \zeta \partial_x f_1(t,x,\zeta) + E(x)\partial_\zeta f_1(t,x,\zeta) = 0, \\ \partial_t f_1(t,x,\zeta) + \zeta \partial_x f_2(t,x,\zeta) + E(x)\partial_\zeta f_2(t,x,\zeta) \\ \qquad\qquad - \dfrac{E(x)}{\zeta}(f_0(t,x,\zeta) - f_2(t,x,\zeta)) = -\dfrac{2\alpha_{ei}(x) f_1(t,x,\zeta)}{\zeta^3}, \end{cases} \tag{1}$$

where f_0, f_1 and f_2 are the first three angular moments of the electron distribution function f. Omitting the x and t dependency, they are given by

$$\begin{aligned} f_0(\zeta) &= \zeta^2 \int_{-1}^{1} f(\mu,\zeta) d\mu, \\ f_1(\zeta) &= \zeta^2 \int_{-1}^{1} f(\mu,\zeta)\mu d\mu, \\ f_2(\zeta) &= \zeta^2 \int_{-1}^{-1} f(\mu,\zeta)\mu^2 d\mu. \end{aligned} \tag{2}$$

The coefficient α_{ei} is a positive physical function which may depend of x, E represents the electrostatic field as function of x and ζ the velocity modulus. The fundamental point of the moments models is the definition of the closure which gives an expression of the highest moment as a function of the lower ones. This closure relation corresponds to an approximation of the underlying distribution function, which the moments system is constructed from. For the M_1 model the closure relation originates from an entropy minimisation principle [41,47]. The moment f_2 can be computed [21,22] as a function of f_0 and f_1

$$f_2(t,x,\zeta) = \chi\Big(\frac{f_1(t,x,\zeta)}{f_0(t,x,\zeta)}\Big) f_0(t,x,\zeta), \qquad \text{with} \qquad \chi(\alpha) = \frac{1+\alpha^2+\alpha^4}{3}. \tag{3}$$

The set of admissible states [21] is defined by

$$\mathcal{A} = \Big((f_0, f_1) \in \mathbb{R}^2, \;\; f_0 \geq 0, \quad |f_1| \leq f_0 \Big). \tag{4}$$

In [31], a numerical scheme was proposed for the electronic M_1 model without electric field and in the homogeneous case. The scheme derived using the consistency with the integral form of the approximate Riemann solver ensures the admissibility conditions (4) and correctly captures the limit diffusion equation. The method proposed in [31] naturally takes into account the source term $-E(x)(f_0 - f_2)/\zeta$, the non linearity of the model which comes from the M_1 model closure and the spatial dependencies of the electric field and the collisional parameter. However, the general model considering the x and ζ dependencies has not been considered. In such a general case, mixed derivatives arise in the diffusion limit leading to complex diffusion equation. In addition, the source term $-E(x)(f_0 - f_2)/\zeta$ also contributes in the limit equation. In this paper, the general electronic M_1 model (1) is considered. The aim is to propose a numerical scheme, extending the ideas of [31], in order to take into account the mixed derivatives in the diffusive limit. Such a scheme must ensure the admissibility conditions (4) and include the contribution of the source term in the diffusion $-E(x)(f_0 - f_2)/\zeta$ limit.

We first introduce the electronic M_1 model with its diffusion limit in Section 2. In Section 3, extending the ideas of [31], a numerical scheme is proposed. The scheme is modified to ensure the admissibility conditions (4) and to capture the non isotropic diffusion then the asymptotic-preserving property is exhibited. The contribution of the term $-E(x)(f_0-f_2)/\zeta$ is finally included in the scheme. In Section 4, numerical examples are presented to testify of the efficiency of the method. Finally, Section 5 presents our conclusions.

2 Model and diffusive limit

In this section, the diffusive limit of the electronic M_1 model is introduced. After considering a diffusive scaling, we use a formal Hilbert expansion to derive the limit model. Even if such a procedure is not strictly rigorous from a mathematical point of view, it is known that this approach gives an easy way to derive the limit model. In addition, mathematical rigorous methods used for continuous descriptions can not be easily adapted in this numerical context.
We consider the following diffusion scaling

$$\tilde{t} = t/t^*, \quad \tilde{x} = x/x^*, \quad \tilde{\zeta} = \zeta/v_{th}, \quad \tilde{E} = Ex^*/v_{th}. \tag{5}$$

The parameters t^* and x^* are chosen such that $\tau_{ei}/t^* = \varepsilon^2$, $\lambda_{ei}/x^* = \varepsilon$, where the electron-ion collisional period is given by $\tau_{ei} = v_{th}^3/(\alpha_{ei}\sigma)$ and the mean free path by $\lambda_{ei} = v_{th}\tau_{ei}$. The coefficient σ depends on the temperature and

the ion density in the plasma. It is a positive function of x and a positive parameter ε, which is devoted to tend to zero. In this case system (1) rewrites

$$\begin{cases} \varepsilon\partial_t f_0(t,x,\zeta) + \zeta\partial_x f_1(t,x,\zeta) + E(x)\partial_\zeta f_1(t,x,\zeta) = 0, \\ \varepsilon\partial_t f_1(t,x,\zeta) + \zeta\partial_x f_2(t,x,\zeta) + E(x)\partial_\zeta f_2(t,x,\zeta) \\ \qquad\qquad - \dfrac{E(x)}{\zeta}(f_0(t,x,\zeta) - f_2(t,x,\zeta)) = -\dfrac{2\sigma(x)}{\zeta^3}\dfrac{f_1(t,x,\zeta)}{\varepsilon}. \end{cases} \tag{6}$$

Introducing the following Hilbert expansion of f_0^ε and f_1^ε

$$\begin{cases} f_0^\varepsilon = f_0^0 + \varepsilon f_0^1 + O(\varepsilon^2), \\ f_1^\varepsilon = f_1^0 + \varepsilon f_1^1 + O(\varepsilon^2), \end{cases} \tag{7}$$

into the second equation of (6) taken at order ε^{-1} leads to

$$f_1^0 = 0. \tag{8}$$

Using the definition of f_2 in (3), it follows that

$$f_2^0 = f_0^0/3. \tag{9}$$

Inserting the Hilbert expansion (7) into the second equation of (1) gives at order ε^0

$$f_1^1 = -\frac{\zeta^4}{6\sigma}\partial_x f_0^0 - \frac{E\zeta^3}{6\sigma}\partial_\zeta f_0^0 + \frac{E\zeta^2}{3\sigma} f_0^0. \tag{10}$$

Finally, using the previous equation in the first equation of (1) at order ε^1, the following limit equation is obtained

$$\begin{aligned} \partial_t f_0^0 + \zeta\partial_x\Big(-\frac{\zeta^4}{6\sigma}\partial_x f_0^0 - \frac{E\zeta^3}{6\sigma}\partial_\zeta f_0^0 + \frac{E\zeta^2}{3\sigma} f_0^0\Big) \\ + E\partial_\zeta\Big(-\frac{\zeta^4}{6\sigma}\partial_x f_0^0 - \frac{E\zeta^3}{6\sigma}\partial_\zeta f_0^0 + \frac{E\zeta^2}{3\sigma} f_0^0\Big) = 0. \end{aligned} \tag{11}$$

In the case $E = 0$, one recognises a classical diffusion equation involving a second order space derivative with a diffusion coefficient of $-\zeta^5/6\sigma$. However, in the general case this limit equation involves mixed x and ζ derivatives leading to a non isotropic diffusion. In addition, the source term $E(f_0 - f_2)/\zeta$ also contributes in the diffusive limit leading to the term $(E\zeta^2/(3\sigma))f_0^0$ in the right side of (10) and in the x and ζ derivatives of (11). Such an asymptotic limit is unusual compared to what has been studied in radiative transfer for example [4,5]. The difference lies in the fact that here charged particles are considered. Then, the contribution of the electric field must be taken into account leading to these unexpected limit involving mixed derivatives.

3 Numerical scheme

The aim of this part is to propose a numerical scheme, generalising the ideas introduced in [31], for the general model (1) and consistent, in the limit ε tends to zero, with equation (11). The main difficulty comes from the derivation of a numerical scheme consistent in the diffusive limit with equation (11) and in particular with the mixed-derivatives. The numerical scheme proposed must also be able to deal with the contribution of the source term $E(f_0 - f_2)/\zeta$.

3.1 Case without the source term $\frac{E}{\zeta}(f_0 - f_2)$

We first consider the case without the source term $\frac{E}{\zeta}(f_0 - f_2)$. With the present approach, it will be seen in part 3.2 that this term can be naturally taken into account. Therefore, for clarity, we start without considering it. Then the electronic M_1 model reads

$$\begin{cases} \partial_t f_0(t,x,\zeta) + \zeta \partial_x f_1(t,x,\zeta) + E(x)\partial_\zeta f_1(t,x,\zeta) = 0, \\ \partial_t f_1(t,x,\zeta) + \zeta \partial_x f_2(t,x,\zeta) + E(x)\partial_\zeta f_2(t,x,\zeta) = -\dfrac{2\sigma(x) f_1(t,x,\zeta)}{\zeta^3} \end{cases} \tag{12}$$

and its diffusive limit equation writes

$$\partial_t f_0^0 + \zeta \partial_x \Big(-\frac{\zeta^4}{6\sigma}\partial_x f_0^0 - \frac{E\zeta^3}{6\sigma}\partial_\zeta f_0^0 \Big) + E\partial_\zeta \Big(-\frac{\zeta^4}{6\sigma}\partial_x f_0^0 - \frac{E\zeta^3}{6\sigma}\partial_\zeta f_0^0 \Big) = 0. \tag{13}$$

3.1.1 Derivation of the scheme

In this part the derivation of an numerical scheme for the model (12) is detailed.
Let us consider an uniform mesh with a constant space step $\Delta x = x_{i+1/2} - x_{i-1/2}$, a constant energy step $\Delta\zeta = \zeta_{i+1/2} - \zeta_{i-1/2}$ and a time step Δt. Extending the ideas introduced in [31], we propose to consider the following numerical scheme

$$\begin{aligned} \frac{U_{ij}^{n+1} - U_{ij}^n}{\Delta t} =& \frac{a_x}{\Delta x} U_{i-1/2j}^{R*} + \frac{2a_x}{\Delta x} U_{ij}^n + \frac{a_x}{\Delta x} U_{i+1/2j}^{L*} \\ &+ \frac{a_\zeta}{\Delta\zeta} U_{ij-1/2}^{R*} + \frac{2a_\zeta}{\Delta\zeta} U_{ij}^n + \frac{a_\zeta}{\Delta\zeta} U_{ij+1/2}^{L*}, \end{aligned} \tag{14}$$

where the intermediate states of the approximated Riemann solver (see Figure 1) $U_{i+1/2j}^{L*}$, $U_{i-1/2j}^{R*}$, $U_{ij+1/2}^{L*}$ and $U_{ij-1/2}^{R*}$ are defined by

$$U_{i-1/2j}^{R*} = \begin{pmatrix} f_{0i-1/2j}^{R*} \\ f_{1i-1/2j}^{*} \end{pmatrix}, \; U_{i+1/2j}^{L*} = \begin{pmatrix} f_{0i+1/2j}^{L*} \\ f_{1i+1/2j}^{*} \end{pmatrix},$$

$$U_{ij-1/2}^{R*} = \begin{pmatrix} f_{0ij-1/2}^{R*} \\ f_{1ij-1/2j}^{*} \end{pmatrix}, \; U_{ij+1/2}^{L*} = \begin{pmatrix} f_{0ij+1/2}^{L*} \\ f_{1ij+1/2}^{*} \end{pmatrix}.$$

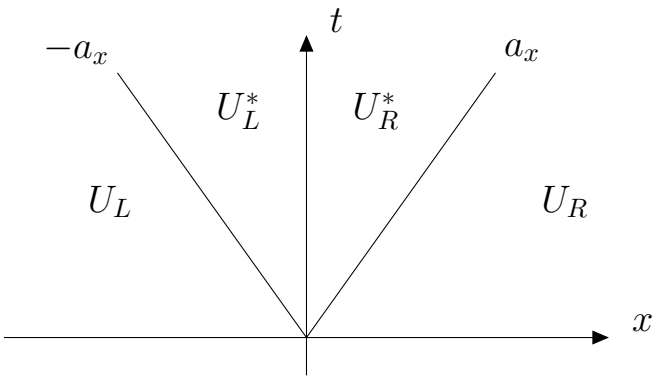

Fig. 1 Structure of the approximate Riemann solver considered.

The second components of the intermediate states at each interface are chosen equal, ie $f^{L*}_{1i+1/2j} = f^{R*}_{1i+1/2j} = f^{*}_{1i+1/2j}$ and $f^{L*}_{1ij+1/2} = f^{R*}_{1ij+1/2} = f^{*}_{1ij+1/2}$.

Following [4,5,31], the velocity waves a_x and a_ζ are fixed such that

$$a_x = \zeta_j, \qquad\qquad a_\zeta = |E_i|. \tag{15}$$

For clarity, in the following, we omit the dependency of the speed a_x in energy and a_ζ in space. However, the results presented hold in the general case. If the intermediate states are defined following [31] the numerical scheme (14) recovers only the second order space and energy derivatives in the diffusive limit. Therefore, in order to take into account the mixed-derivative terms in the diffusive limit leading to an anisotropic diffusion, we propose to modify the numerical viscosity of the intermediate state f_1^* used in [31] in the following way

$$f^{*}_{1i+1/2j} = \alpha_{i+1/2j}\Big[\frac{f_{1i+1j}+f_{1ij}}{2} - \frac{1}{2a_x}(\zeta_j f_{2i+1j} - \zeta_j f_{2ij}) - c_{i+1/2j}(\frac{\partial f_0}{\partial \zeta})_{i+1/2j}(1-\alpha_{i+1/2j})\Big], \tag{16}$$

$$f^{*}_{1ij+1/2} = \beta_{ij+1/2}\Big[\frac{f_{1ij+1}+f_{1ij}}{2} - \frac{1}{2a_\zeta}(E_i f_{2ij+1} - E_i f_{2ij}) - \bar{c}_{ij+1/2}(\frac{\partial f_0}{\partial x})_{ij+1/2}(1-\beta_{ij+1/2})\Big], \tag{17}$$

with

$$\alpha_{i+1/2j} = \frac{2a_x\zeta_j^3}{2a_x\zeta_j^3 + \sigma_{i+1/2}\Delta x}, \qquad \beta_{ij+1/2} = \frac{2a_\zeta\zeta_{j+1/2}^3}{2a_\zeta\zeta_{j+1/2}^3 + \sigma_i\Delta\zeta}. \tag{18}$$

In this case, the numerical viscosity contributes in the x and ζ directions. The terms $(\frac{\partial f_0}{\partial \zeta})_{i+1/2j}$, $(\frac{\partial f_0}{\partial x})_{ij+1/2}$ and the coefficients c and $\bar{c}$ are fixed in order to obtain the relevant limit equation (11) in the diffusion regime. We set

$$c_{i+1/2j} = \frac{E_{i+1/2}\Delta x}{3a_x}, \qquad \bar{c}_{ij+1/2} = \frac{\zeta_{j+1/2}\Delta\zeta}{3a_\zeta}. \tag{19}$$

We use an upwind scheme for the discretisation of the terms $(\frac{\partial f_0}{\partial \zeta})_{i+1/2j}$ and $(\frac{\partial f_0}{\partial x})_{ij+1/2}$. The coefficient $\bar{c}$ is always positive then

$$\bar{c}_{ij+1/2}(\frac{\partial f_0}{\partial x})_{ij+1/2} \approx \bar{c}_{ij+1/2}\frac{f_{0i+1j+1} - f_{0ij+1} + f_{0i+1j} - f_{0ij}}{2\Delta x},$$

$$c_{i+1/2j}(\frac{\partial f_0}{\partial \zeta})_{i+1/2j} \approx \begin{cases} c_{i+1/2j}\dfrac{f_{0i+1j} - f_{0i+1j-1} + f_{0ij} - f_{0ij-1}}{2\Delta\zeta} & \text{if } c_{i+1/2j} < 0, \\ c_{i+1/2j}\dfrac{f_{0i+1j+1} - f_{0i+1j} + f_{0ij+1} - f_{0ij}}{2\Delta\zeta} & \text{if } c_{i+1/2j} > 0. \end{cases}$$

The previous two conditions rewrite

$$\begin{aligned} c_{i+1/2j}(\frac{\partial f_0}{\partial \zeta})_{i+1/2j} = {} & c^-_{i+1/2j}\frac{f_{0i+1j} - f_{0i+1j-1} + f_{0ij} - f_{0ij-1}}{2\Delta\zeta} \\ & + c^+_{i+1/2j}\frac{f_{0i+1j+1} - f_{0i+1j} + f_{0ij+1} - f_{0ij}}{2\Delta\zeta}, \end{aligned}$$

with $(c)^+ = \max(c, 0)$ and $(c)^- = \min(c, 0)$.

We introduce the following notations

$$\begin{aligned} \tilde{f}_{0i+1/2j} &= \frac{f_{1i+1j} + f_{1ij}}{2} - \frac{(\zeta_j f_{2i+1j} - \zeta_j f_{2ij})}{2a_x(2 - \alpha_{i+1/2j})}, \\ \tilde{f}_{1i+1/2j} &= \frac{f_{1ij+1} + f_{1ij}}{2} - \frac{(E_i f_{2ij+1} - E_i f_{2ij})}{2a_\zeta(2 - \beta_{ij+1/2})}. \end{aligned} \tag{20}$$

In [31], the intermediate states of the considered approximate Riemann solvers were defined using consistency relations and a corrective coefficient to ensure the admissibility conditions. Extending these ideas, the intermediate states $f^{R*}_{0i+1/2j}$ and $f^{L*}_{0i+1/2j}$ are defined by

$$\begin{cases} f^{L*}_{0i+1/2j} = \tilde{f}_{0i+1/2j} - \Gamma_{i+1/2j}\theta_{1i+1/2j}, \\ f^{R*}_{0i+1/2j} = \tilde{f}_{0i+1/2j} + \Gamma_{i+1/2j}\theta_{1i+1/2j}, \end{cases} \tag{21}$$

with

$$\Gamma_{i+1/2j} = \frac{1}{2}[f_{0i+1j} - f_{0ij} - \frac{\zeta_j}{a_x}(f_{1ij} - 2f^*_{1i+1/2j} + f_{1i+1j})], \tag{22}$$

and the coefficient $\theta_{1i+1/2j}$ is fixed in order to ensure the admissibility conditions (4). Similarly, the definitions of $f^{R*}_{0ij+1/2}$ and $f^{L*}_{0ij-1/2}$ read

$$\begin{cases} f^{L*}_{0ij+1/2} = \tilde{f}_{0ij+1/2} - \Gamma_{ij+1/2}\theta_{2ij+1/2}, \\ f^{R*}_{0ij+1/2j} = \tilde{f}_{0ij+1/2} + \Gamma_{ij+1/2}\theta_{2ij+1/2}, \end{cases} \tag{23}$$

with

$$\Gamma_{ij+1/2} = \frac{1}{2}[f_{0ij+1} - f_{0ij} - \frac{\zeta_j}{a_\zeta}(f_{1ij} - 2f^{\star}_{1ij+1/2} + f_{1ij+1})].$$

In order to ensure the admissibility conditions (4), the definitions of the intermediate states $f^{*}_{1i+1/2j}$ and $f^{*}_{1ij+1/2}$ given in (16) and (17) are modified such that

$$f^{*}_{1i+1/2j} = \alpha_{i+1/2j}\Big[\tilde{f}_{1i+1/2j} - \theta_{1i+1/2j}c_{i+1/2j}(\frac{\partial f_0}{\partial \zeta})_{i+1/2j}(1-\alpha_{i+1/2j})\Big], \tag{24}$$

$$f^{*}_{1ij+1/2} = \beta_{ij+1/2}\Big[\tilde{f}_{1ij+1/2} - \theta_{2ij+1/2}\bar{c}_{ij+1/2}(\frac{\partial f_0}{\partial x})_{ij+1/2}(1-\beta_{ij+1/2})\Big]. \tag{25}$$

Remark 1 In the case $\theta_{1i+1/2j} = 0$ and $\theta_{2ij+1/2} = 0$, the admissibility requirements (4) are fulfilled.

Then $\theta_{1i+1/2j}$ and $\theta_{2ij+1/2}$ are fixed in the interval $[0,1]$, the larger possible such that the admissibility requirements (4) are fulfilled. A simple calculation gives the following conditions

$$\tilde{\theta}_{1i+1/2j} = \frac{\tilde{f}_{0i+1/2j} - \alpha_{i+1/2j}|\tilde{f}_{1i+1/2j}|}{|\Gamma_{i+1/2j}| + |\alpha_{i+1/2j}(\frac{\partial f_0}{\partial \zeta})_{i+1/2j}c_{i+1/2j}|}, \tag{26}$$

and

$$\tilde{\theta}_{2ij+1/2} = \frac{\tilde{f}_{0ij+1/2} - \beta_{ij+1/2}|\tilde{f}_{1ij+1/2}|}{|\Gamma_{ij+1/2}| + |\beta_{ij+1/2}(\frac{\partial f_0}{\partial \zeta})_{ij+1/2}\bar{c}_{ij+1/2}|}. \tag{27}$$

Finally, $\theta_{1i+1/2j} = \min(\tilde{\theta}_{1i+1/2j}, 1)$ and $\theta_{2ij+1/2} = \min(\tilde{\theta}_{2ij+1/2}, 1)$.

Theorem 1 *(Admissibility) If for all $(i,j) \in \mathbb{N}^2$, $U^n_{i,j} \in \mathcal{A}$, then for all $(i,j) \in \mathbb{N}^2$, $U^{n+1}_{i,j} \in \mathcal{A}$ as soon as the following CFL condition holds*

$$\Delta t \leq \frac{\Delta\zeta\Delta x}{(2a_x\Delta\zeta + 2a_\zeta\Delta x)}.$$

Proof The numerical scheme (14) also writes as a convex combination of vectors of $\mathcal{A}$

$$\begin{aligned} U_{ij}^{n+1} =&(1-\frac{2a_x\Delta t}{\Delta x}-\frac{2a_\zeta\Delta t}{\Delta\zeta})U_{ij}^{n}+\frac{a_x\Delta t}{\Delta x}U_{i-1/2j}^{R*}+\frac{a_x\Delta t}{\Delta x}U_{i+1/2j}^{L*} \\ &+\frac{a_\zeta\Delta t}{\Delta\zeta}U_{ij-1/2}^{R*}+\frac{a_\zeta\Delta t}{\Delta\zeta}U_{ij+1/2}^{L*}, \end{aligned} \tag{28}$$

Using the definitions of θ_1 and θ_2 given in (26) and (27) the intermediate states $U_{i-1/2j}^{R*}$, $U_{i+1/2j}^{L*}$, $U_{ij-1/2}^{R*}$ and $U_{ij+1/2}^{L*}$ belong to $\mathcal{A}$. Since $\mathcal{A}$ is a convex space it follows that the updated states U_i^{n+1} belongs to $\mathcal{A}$.

3.1.2 Asymptotic-preserving properties

In this part, the consistency in the classical regime and the asymptotic-preserving property of the scheme in the diffusive regime are exhibited.

Theorem 2 *(Consistency in the classical regime) The numerical scheme (14) is consistent, when Δt and Δx tend to zero, with the set of equations (12).*

Proof Using the definitions (16) and (17), the second component of (14) reads

$$\begin{aligned} \frac{f_{1ij}^{n+1}-f_{1ij}^{n}}{\Delta t} =&\frac{a_x}{\Delta x}\Big[\alpha_{i+1/2j}\Big(\tilde{f}_{1i+1/2j}-\theta_{1i+1/2j}c_{i+1/2j}(\frac{\partial f_0}{\partial\zeta})_{i+1/2j}(1-\alpha_{i+1/2j})\Big)\Big] \\ &-\frac{2a_x}{\Delta x}f_{1ij}^{n} \\ &+\frac{a_x}{\Delta x}\Big[\alpha_{i-1/2j}\Big(\tilde{f}_{1i-1/2j}-\theta_{1i-1/2j}c_{i-1/2j}(\frac{\partial f_0}{\partial\zeta})_{i-1/2j}(1-\alpha_{i-1/2j})\Big)\Big] \\ &+\frac{a_\zeta}{\Delta\zeta}\Big[\beta_{ij+1/2}\Big(\tilde{f}_{1ij+1/2}-\theta_{2ij+1/2}\bar{c}_{ij+1/2}(\frac{\partial f_0}{\partial x})_{ij+1/2}(1-\beta_{ij+1/2})\Big)\Big] \\ &-\frac{2a_\zeta}{\Delta\zeta}f_{1ij}^{n} \\ &+\frac{a_\zeta}{\Delta\zeta}\Big[\beta_{ij-1/2}\Big(\tilde{f}_{1ij-1/2}-\theta_{2ij-1/2}\bar{c}_{ij-1/2}(\frac{\partial f_0}{\partial x})_{ij-1/2}(1-\beta_{ij-1/2})\Big)\Big]. \end{aligned} \tag{29}$$

Inserting the definitions (20) into (29) and using the following expressions for $\alpha_{i+1/2j}$ and $\beta_{ij+1/2}$

$$\alpha_{i+1/2j}=\frac{2a_x\zeta_j^3}{2a_x\zeta_j^3+\sigma_{i+1/2}\Delta x}=1-\frac{\sigma_{i+1/2}\Delta x}{2a_x\zeta_j^3+\sigma_{i+1/2}\Delta x},$$

and

$$\beta_{ij+1/2}=\frac{2a_\zeta\zeta_{j+1/2}^3}{2a_\zeta\zeta_{j+1/2}^3+\sigma_i\Delta\zeta}=1-\frac{\sigma_i\Delta\zeta}{2a_\zeta\zeta_{j+1/2}^3+\sigma_i\Delta\zeta},$$

lead to the consistency with the second equation of (12) as Δx and Δt tend to zero. A similar calculation gives the consistency with the first equation of (12).

Theorem 3 *(Consistency in the diffusive regime)*

In the diffusive limit, the numerical scheme (14) degenerates into

$$\begin{aligned}\frac{f_{0ij}^{n+1,0}-f_{0ij}^{n,0}}{\Delta t} =&\frac{\zeta_j}{\Delta x}\Big[\frac{\zeta_j^4}{6\sigma_{i+1/2}\Delta x}(f_{0i+1j}^{n,0}-f_{0ij}^{n,0})-\frac{\zeta_j^4}{6\sigma_{i-1/2}\Delta x}(f_{0i1j}^{n,0}-f_{0i-1j}^{n,0})\\ &+\frac{\zeta_j^3 E_{i+1/2}}{6\sigma_{i+1/2}}(\frac{\partial f_0^{n,0}}{\partial\zeta})_{i+1/2j}-\frac{\zeta_j^3 E_{i-1/2}}{6\sigma_{i-1/2}}(\frac{\partial f_0^{n,0}}{\partial\zeta})_{i-1/2j}\Big]\\ &+\frac{E_i}{\Delta\zeta}\Big[\frac{E_i\zeta_{j+1/2}^3}{6\sigma_i\Delta\zeta}(f_{0ij+1}^{n,0}-f_{0ij}^{n,0})-\frac{E_i\zeta_{j-1/2}^3}{6\sigma_i\Delta\zeta}(f_{0i1j}^{n,0}-f_{0ij-1}^{n,0})\\ &+\frac{\zeta_{j+1/2}^4}{6\sigma_i}(\frac{\partial f_0^{n,0}}{\partial x})_{ij+1/2}-\frac{\zeta_{j-1/2}^4}{6\sigma_i}(\frac{\partial f_0^{n,0}}{\partial x})_{ij-1/2}\Big].\end{aligned}\tag{30}$$

Proof Following the same approach as in [5,7,31], using the diffusive scaling and equation (14) leads to

$$\begin{aligned}\varepsilon\frac{U_{ij}^{n+1,\varepsilon}-U_{ij}^{n,\varepsilon}}{\Delta t} =&\frac{a_x}{\Delta x}U_{i-1/2j}^{R*,\varepsilon}-\frac{2a_x}{\Delta x}U_{ij}^{n,\varepsilon}+\frac{a_x}{\Delta x}U_{i+1/2j}^{L*,\varepsilon}\\ &+\frac{a_\zeta}{\Delta\zeta}U_{ij-1/2}^{R*,\varepsilon}-\frac{2a_\zeta}{\Delta\zeta}U_{ij}^{n,\varepsilon}+\frac{a_\zeta}{\Delta\zeta}U_{ij+1/2}^{L*,\varepsilon},\end{aligned}\tag{31}$$

and equations (24) and (25) give

$$\begin{aligned}f_{1i+1/2j}^{*,\varepsilon}&=\alpha_{i+1/2j}^{\varepsilon}\Big[\tilde{f}_{1i+1/2j}^{\varepsilon}-\theta_{1i+1/2j}c_{i+1/2j}(\frac{\partial f_0^{\varepsilon}}{\partial\zeta})_{i+1/2j}(1-\alpha_{i+1/2j}^{\varepsilon})\Big],\\ f_{1ij+1/2}^{*,\varepsilon}&=\beta_{ij+1/2}^{\varepsilon}\Big[\tilde{f}_{1ij+1/2}^{\varepsilon}-\theta_{2ij+1/2}\bar{c}_{ij+1/2}(\frac{\partial f_0^{\varepsilon}}{\partial x})_{ij+1/2}(1-\beta_{ij+1/2}^{\varepsilon})\Big],\end{aligned}\tag{32}$$

with

$$\alpha_{i+1/2j}^{\varepsilon}=\frac{2a_x\zeta_j^3}{2a_x\zeta_j^3+\sigma_{i+1/2}\Delta x/\varepsilon},\qquad \beta_{ij+1/2}^{\varepsilon}=\frac{2a_\zeta\zeta_{j+1/2}^3}{2a_\zeta\zeta_{j+1/2}^3+\sigma_i\Delta\zeta/\varepsilon}.\tag{33}$$

Then it follows that

$$f_{1i+1/2j}^{*,0}=0\qquad\text{and}\qquad f_{1ij+1/2}^{*,0}=0.$$

The second component of (31) reads

$$\begin{aligned}\varepsilon\frac{f_{1ij}^{n+1,\varepsilon}-f_{1ij}^{n,\varepsilon}}{\Delta t} =&\frac{a_x}{\Delta x}f_{1i-1/2j}^{*,\varepsilon}-\frac{2a_x}{\Delta x}f_{1ij}^{n,\varepsilon}+\frac{a_x}{\Delta x}f_{1i+1/2j}^{*,\varepsilon}\\ &+\frac{a_\zeta}{\Delta\zeta}f_{1ij-1/2}^{*,\varepsilon}-\frac{2a_\zeta}{\Delta\zeta}f_{1ij}^{n,\varepsilon}+\frac{a_\zeta}{\Delta\zeta}f_{1ij+1/2}^{*,\varepsilon}.\end{aligned}$$

At order ε^0 the previous equation leads to

$$f_{1ij}^{n,0} = 0. \tag{34}$$

In the limit ε tends to zero, the results (3.1.2) and (34) give

$$\theta_{1i+1/2j} = 1, \qquad \theta_{2ij+1/2} = 1. \tag{35}$$

Indeed, when ε tends to zero, the definitions (26) and (27) lead to

$$\tilde{\theta}_{1i+1/2j} = \frac{f_{0i+1j}^{n,0} + f_{0ij}^{n,0}}{|f_{0i+1j}^{n,0} - f_{0ij}^{n,0}|} \geq 1, \qquad \tilde{\theta}_{2ij+1/2} = \frac{f_{0ij+1}^{n,0} + f_{0ij}^{n,0}}{|f_{0ij+1}^{n,0} - f_{0ij}^{n,0}|} \geq 1.$$

The first component of (31) reads

$$\begin{aligned}\varepsilon\frac{f_{0ij}^{n+1,\varepsilon} - f_{0ij}^{n,\varepsilon}}{\Delta t} =& \frac{a_x}{\Delta x} f_{0i-1/2j}^{R*,\varepsilon} - \frac{2a_x}{\Delta x} f_{0ij}^{n,\varepsilon} + \frac{a_x}{\Delta x} f_{0i+1/2j}^{L*,\varepsilon} \\ &+ \frac{a_\zeta}{\Delta \zeta} f_{0ij-1/2}^{R*,\varepsilon} - \frac{2a_\zeta}{\Delta \zeta} f_{0ij}^{n,\varepsilon} + \frac{a_\zeta}{\Delta \zeta} f_{0ij+1/2}^{L*,\varepsilon}.\end{aligned}$$

Using the definitions (21) and (23), the result (35) and the previous equation considered at order ε^1 gives the numerical scheme (30).

3.2 General case with the term $\frac{E}{\zeta}(f_0 - f_2)$

As specified in part 3.1, in order to take into account the contribution of the source term $\frac{E}{\zeta}(f_0 - f_2)$, we simply propose to modify the intermediate states $f_{1i+1/2j}^*$ and $f_{1ij+1/2}^*$ given in (24) and (25) such that

$$f_{1i+1/2j}^* = \alpha_{i+1/2j}\Big[\tilde{f}_{1i+1/2j} - \theta_{1i+1/2j} c_{i+1/2j}\Big((\frac{\partial f_0}{\partial \zeta})_{i+1/2j} - \frac{\tilde{S}_{i+1/2j}}{2}\Big)(1 - \alpha_{i+1/2j})\Big], \tag{36}$$

$$f_{1ij+1/2}^* = \beta_{ij+1/2}\Big[\tilde{f}_{1ij+1/2} + \frac{\Delta\zeta}{2a_\zeta} S_{ij+1/2} - \theta_{2ij+1/2}\bar{c}_{ij+1/2}(\frac{\partial f_0}{\partial x})_{ij+1/2}(1 - \beta_{ij+1/2})\Big],$$

with

$$\tilde{S}_{i+1/2j} = \frac{\zeta_j^2}{3\sigma_i}\frac{f_{0i+1j} + f_{0ij}}{2} \quad \text{and} \quad S_{ij+1/2} = \frac{E_i}{2}\Big(\frac{f_{0ij+1} - f_{2ij+1}}{\zeta_{j+1}} + \frac{f_{0ij} - f_{2ij}}{\zeta_j}\Big).$$

In this case, as in the previous part the coefficients θ_1 and θ_2 are also fixed to ensure the admissibility requirements.

Theorem 4 *In the diffusive limit, the numerical scheme given by (14)-(21)-(23)-(36) is consistent with the limit equation (11).*

Proof The proof is the same than for Theorem 3, considering the intermediate states $f^*_{1i+1/2j}$ and $f^*_{1ij+1/2}$ given in (36). A direct calculation using the Hilbert expansions leads to the result. The terms $S_{ij+1/2}$ are consistent with the term $\frac{E}{\zeta}(f_0 - f_2)$ while the terms $\tilde{S}_{i+1/2j}$ enable to correctly recover the contribution of the two terms $\frac{E\zeta^2}{3\sigma} f_0$ in the x and ζ derivatives of the limit equation.

4 Numerical examples

In this section, the asymptotic-preserving scheme (14) is compared with the HLL scheme and an explicit discretisation of the diffusion equation (11) in the diffusive regime.

4.1 Relaxation of a Gaussian profile in the diffusive regime

In this example, the numerical scheme (14)-(21)-(23)-(36) is validated in the diffusive regime considering an inhomogeneous plasma with electric field. In this case, the initial conditions are the following

$$\begin{cases} f_0(t=0,x,\zeta) = \zeta^2 \exp(-x^2) \exp(2(\zeta-3)^2), \\ f_1(t=0,x,\zeta) = 0. \end{cases}$$

The profile of f_0 at initial time as a function of x and ζ is displayed in Figure 2.

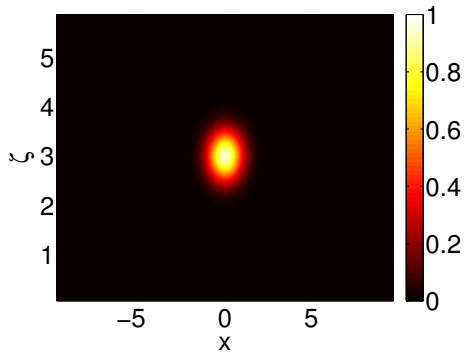

Fig. 2 Representation of the f_0 profile at the initial time as a function of x and ζ.

For this test we have set $E = 1$, $\sigma = 10^4$, the space range chosen is [-10,10] and the energy range [0,6]. In Figure 3, the solution obtained with the numerical scheme (14)-(21)-(23)-(36) is compared with the solution obtained with the HLL scheme and with an explicit discretisation of the limit diffusion equation

(11) at different times. At time $t = 1$, one remarks that the f_0 profile obtained with the HLL scheme is already seriously spread out while the profiles obtained with the AP scheme and the diffusion equation do not have changed. At time $t = 50$, the AP scheme and diffusion equation discretisation f_0 profiles are spread out while the profile obtained with the HLL scheme has vanished. As observed at time t=100, in the long time regime, the AP scheme and the discretisation of the diffusion equation behave identically.

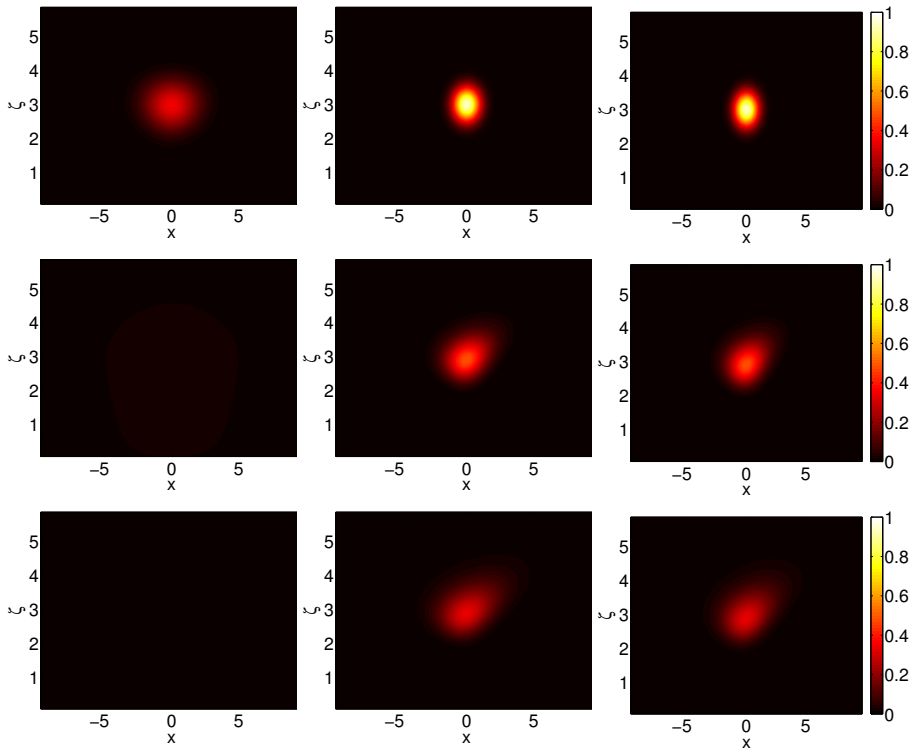

Fig. 3 Representation of the f_0 profile as function of x and ζ at time t=1 (top), t=50 (middle), t=100 (bottom), for the HLL scheme (left), AP scheme (middle) and the diffusion equation.

4.2 Relaxation of a temperature profile in the diffusive regime with a self-consistent electric field

In this example, we consider the relaxation of a temperature profile in the diffusive regime considering a self-consistent electric field. The space range is $[-40, 40]$ and the energy range $[0, 6]$. The initial conditions are the following

$$\begin{cases} f_0(t=0,x,\zeta) = \sqrt{\dfrac{2}{\pi}} \dfrac{\zeta^2}{T^{ini}(x)^{3/2}} \exp(-\dfrac{\zeta^2}{2T^{ini}(x)}), \\ f_1 = 0, \end{cases} \tag{37}$$

with $T^{ini}(x) = 2 - \arctan(x)$.

In this case the electric field is self-consistent meaning that at each time step it is calculated from the plasma profile. In this case we consider a Spitzer type model [55,9], to evaluate the electric field

$$E(x) = -\frac{dT(x)}{dx}, \tag{38}$$

where

$$T(x) = \frac{1}{3n_e}\Big(\int_0^{+\infty} \zeta^2 f_0 d\zeta - u^2 n_e\Big),$$

with $n_e = \int_0^{+\infty} f_0 d\zeta$ and $u = \frac{1}{n_e}\int_0^{+\infty} f_1 \zeta d\zeta$.

In Figure 4, the temperature profile is displayed at the initial time and at time t=80. The temperature profiles obtained with the HLL scheme, the AP scheme and a discretisation of the diffusion equation (11) are compared at time t=80. On one hand, one remarks that the HLL temperature profile is excessively spread out compared to the AP and diffusion profiles while on the other hand the AP and diffusion profiles match exactly at time t=80. This example demonstrates the inability of the HLL scheme in capturing the correct temperature profile while the AP scheme presented handle perfectly the diffusive limit regime.

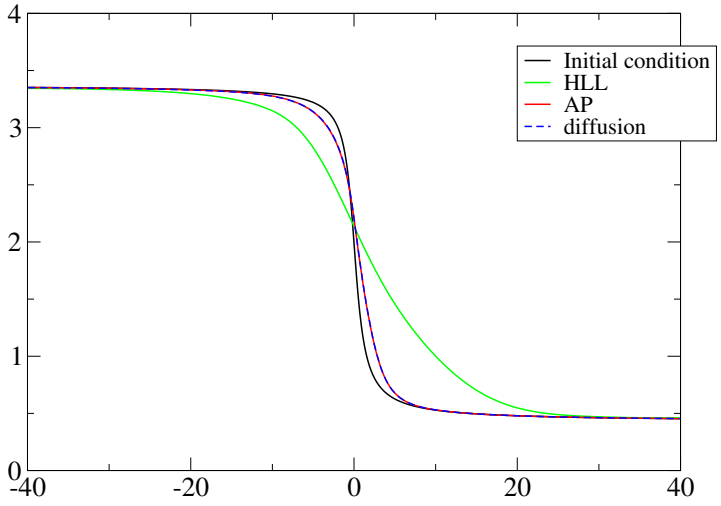

Fig. 4 Representation of the temperature profile as a function of x at time t=80.

4.3 Two electron beams interaction

In this example the interaction between two electron beams is considered. This collisionless test case enables us to validate the AP scheme (14)-(21)-

(23)-(36) in a regime where electrostatic effects are predominant compared to the collisional effects, therefore we set $\sigma = 0$.
Consider two electron beams propagating at velocity v_0 and v_1. In that case, the dispersion relation [34] is given by

$$1 - \frac{1}{(\omega - kv_0)^2} - \frac{1}{(\omega - kv_1)^2} = 0,$$

where v_0 and v_1 denote the beams velocities.

This configuration can lead to electrostatic instabilities [18,34]. Indeed, the solutions of the form $Ae^{i\omega t + ikx}$ are unstable when ω_I the imaginary part of ω is strictly positive. In the case $v_0 = -v_1$ we can show that the solution is stable if $kv_0 \geq \sqrt{2}$.

This test is problematic for the M_1 model. Indeed, if we consider two electron beams propagating with opposite velocities the distribution function is well defined. Nevertheless, the M_1 model considers only the angular moments f_0 and f_1. For the calculation of f_1 the two populations contributions cancel and we get $f_1 = 0$. The M_1 model sees an unrealistic isotropic configuration. To overcome this problem the superposition principle is used since the model is linear [58,34]. Two particle populations (one per beam) are considered. For each time step the M_1 problem is solved for the first population then for the second one. Hence the electrostatic field is calculated using the Maxwell-Ampere solved taking into account the two distribution functions. This approach was validated for the present test case in [32].

In the case of two streams propagating with opposite velocities v_d and $-v_d$, the initial electron distribution function is the following

$$f(t = 0, x, v) = 0.5[(1 + A\cos(kx))M_{v_d}(v) + (1 - A\cos(kx))M_{-v_d}(v)],$$

with

$$M_{\pm v_d}(v) = \exp\Big(-\frac{(v \mp v_d)^2}{2}\Big).$$

The first corresponding angular moments f_0^1 and f_0^2 of the first and second population read

$$\begin{cases} f_0^1(t = 0, x, \zeta) = 0.5(1 + A\cos(kx))\dfrac{\zeta}{v_d}\Big(\exp(-\dfrac{(\zeta - v_d)^2}{2}) - \exp(-\dfrac{(\zeta + v_d)^2}{2})\Big), \\ f_0^2(t = 0, x, \zeta) = 0.5(1 - A\cos(kx))\dfrac{\zeta}{v_d}\Big(\exp(-\dfrac{(\zeta - v_d)^2}{2}) - \exp(-\dfrac{(\zeta + v_d)^2}{2})\Big). \end{cases}$$

The second angular moments f_1^1 and f_1^2 of the first and second population read

$$\begin{cases} f_1^1(t = 0, x, \zeta) = 0.5(1 + A\cos(kx))\dfrac{1 - \zeta v_d}{v_d^2}\Big(\exp(-\dfrac{(\zeta - v_d)^2}{2}) - \exp(-\dfrac{(\zeta + v_d)^2}{2})\Big), \\ f_1^2(t = 0, x, \zeta) = -0.5(1 - A\cos(kx))\dfrac{1 - \zeta v_d}{v_d^2}\Big(\exp(-\dfrac{(\zeta - v_d)^2}{2}) - \exp(-\dfrac{(\zeta + v_d)^2}{2})\Big). \end{cases}$$

At each time step, the electrostatic field is computed using the Maxwell-Ampere equation considering the contribution of the two population of particles

$$\frac{dE}{dt} = \int_0^{+\infty} f_1^1 \zeta d\zeta + \int_0^{+\infty} f_1^2 \zeta d\zeta.$$

The parameter A is introduced to perturb the initial condition in order to enable the development of the electrostatic instability. The energy range chosen is [0,12] and the space range is [0,25]. In this example we set $v_d = 4$, $A = 0.001$ and periodical boundary conditions are used. The results have been compared with a kinetic code [24]. In Figure 5, the evolution of the electrostatic energy is displayed as a function of time using the AP scheme in red and the kinetic code in dashed blue. The AP scheme and the kinetic code give analogous results. This numerical experiment shows the good behaviour of the AP scheme in a regime where electrostatic effects are predominant.

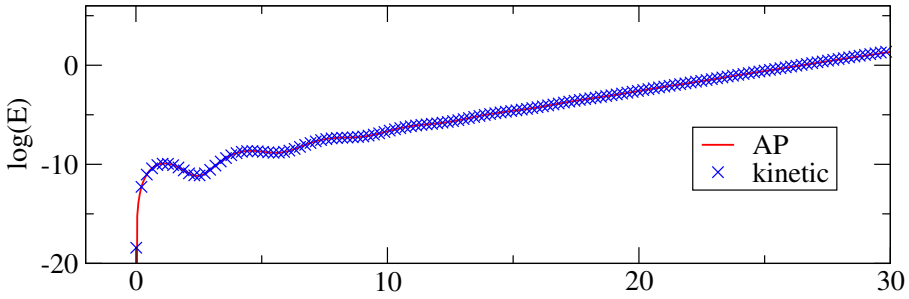

Fig. 5 Representation of the temporal evolution of the electrostatic energy.

4.4 Relaxation of a temperature profile in the diffusive regime with a self-consistent electric field and non-constant collisional parameter

In this example, the initial conditions are the same than for the previous example where the initial temperature profile is given by (37) and the electric field is computed using (38). In this case the collisional parameter σ is not constant and follows the linear profile

$$\sigma(x) = ax + b,$$

with $\sigma(x_{min} = -40) = 5 \cdot 10^3$ and $\sigma(x_{max} = 40) = 10^5$. It follows that the coefficients a and b read

$$a = \frac{10^5 - 5.10^3}{x_{max} - x_{min}}, \qquad b = 5.10^3 - a x_{min}.$$

The space range is [-40,40] and the energy range [0,6]. In Figure 6, the temperature profile is displayed at the initial time and at time t=5000 for the AP

scheme and an explicit discretisation of the diffusion equation (11). After a long time (t=5000) and despite the strong spatial variation of the function σ the AP and diffusion profiles give very close result. One remark on the space interval [-40,0] the AP curve in red is slightly different to the diffusion curve in dashed blue while on the interval [0,40] the results match perfectly. This could be explained as the collisional parameter σ becomes larger for important x, therefore, the limit diffusive regime is fully reached for large x where the comparison with the diffusion equation is valid.

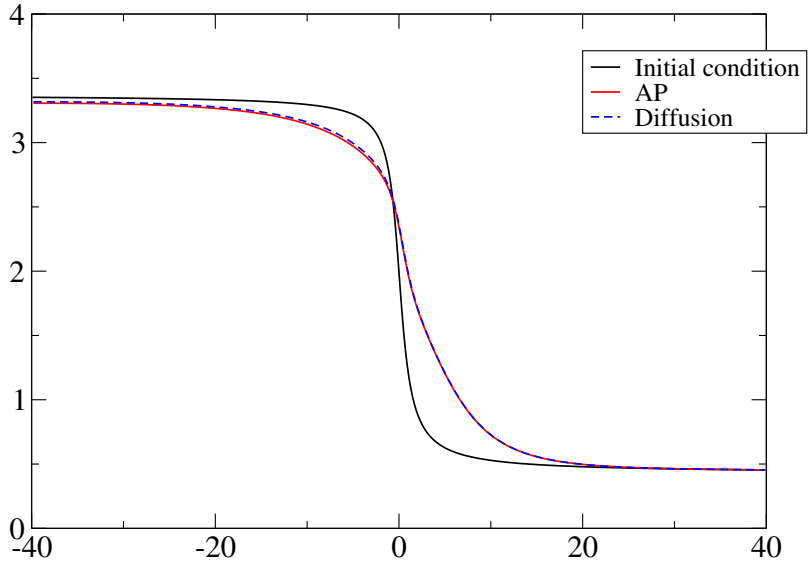

Fig. 6 Representation of the temperature profile at time t=5000.

4.5 Case a non-constant self-consistent collisional parameter

When considering physical relevant configurations occurring in plasma physics, the collisional parameter depends of the state of the plasma. The knowledge of the ionic and electronic distribution function is required to compute the collisional parameter. Therefore in this test case, we choose to consider a nonlinear collisional parameter which depends of the solution itself

$$\sigma(t,x,\zeta) = \exp(f_0(t,x,\zeta) + f_1(t,x,\zeta)).$$

In this case, $E = 1$, the space range chosen is [-10,10] and the energy range [0,6]. The initial condition is given by

$$\begin{cases} f_0(t=0,x,\zeta) = \zeta^2 \exp(-(\zeta-3)^2)) \exp(-x^2/10), \\ f_1 = 0. \end{cases}$$

We consider periodical boundary conditions. In Figure 7, the initial profile of f_0 is displayed at the initial time and at time t=3.

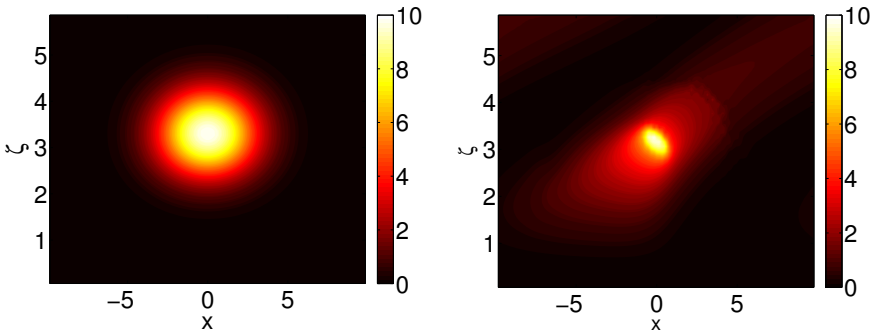

Fig. 7 Representation of the f_0 profile as function of x and ζ at the initial time (left) and t=3 (right).

5 Conclusion

In this work, an asymptotic-preserving scheme has been proposed for the electronic M_1 model in the diffusive limit. In order to deal with the mixed derivatives which arise in the diffusive limit an anisotropic numerical viscosity has been considered. The numerical scheme preserves the realisibility domain and captures the correct limit equation. The contribution of the source term $E(f_0 - f_2)/\zeta$ is integrated and the cases of non constant electric field and collisional parameter are naturally included. Numerical examples have been performed in non-collisional and diffusive regimes. It has been observed that the present scheme behaves correctly in both regimes.
A possible perspective could be to consider an electron-electron collisional operator or the study of the coupling with the Maxwell's equations.

References

1. G.W. Alldredge, C.D. Hauck, and A.L. Tits. High-order entropy-based closures for linear transport in slab geometry II: A computational study of the optimization problem. SIAM Journal on Scientific Computing Vol. 34-4 (2012), pp. B361-B391.
2. D. Aregba-Driollet, M. Briani, and R. Natalini. Asymptotic High-Order Schemes for 2x2 Dissipative Hyperbolic Systems. SIAM Journal on Numerical Analysis 46 (2008), 869-894.
3. R. Balescu. Transport Processes in Plasma, Elsevier, (Amsterdam, 1988), Vol. 1.
4. C. Berthon, P. Charrier, and B. Dubroca. An asymptotic preserving relaxation scheme for a moment model of radiative transfer. C. R. Acad. Sci. Paris, Ser. I 344 (2007).

5. C. Berthon, P. Charrier, and B. Dubroca. An HLLC Scheme to Solve The M1 Model of Radiative Transfer in Two Space Dimensions. Journal of Scientific Computing, Vol. 31, No. 3, (2007).
6. C. Berthon, G. Moebs, and R. Turpault. An Asymptotic-Preserving Scheme for Systems of Conservation Laws with Source Terms on 2D Unstructured Meshes. Finite Volumes for Complex Applications VII-Methods and Theoretical Aspects Volume 77 of the series Springer Proceedings in Mathematics and Statistics pp 107-115.
7. C. Berthon and R.Turpault. Asymptotic preserving HLL schemes. Numerical Methods for Partial Differential Equations, 27 (6) (2011) 1396-1422.
8. F. Bouchut, H. Ounaissa, and B. Perthame. Upwinding of the source term at interfaces for Euler equations with high friction. Computers and Mathematics with Applications 53 (2007), 361-375.
9. S.I. Braginskii. Reviews of Plasma Physics. M.A Leontovich, Ed., Consultants Bureau (New York, 1965), Vol. 1, p.205.
10. A.V. Brantov, V.Yu. Bychenkov, O.V. Batishchev, and W.Rozmus. Nonlocal heat wave propagation due to skin layer plasma heating by short laser pulses. Computer Physics communications 164 67, (2004).
11. C. Buet and S. Cordier. Conservative and entropy decaying numerical scheme for the isotropic Fokker-Planck-Landau equation. J. Comput. Phys. 145, No.1, 228-245 (1998).
12. C. Buet and B. Després. Asymptotic preserving and positive schemes for radiation hydrodynamics. J. Compt. Phy., 215, 717740 (2006).
13. C. Buet, B. Desprs, and E. Franck. Design of asymptotic preserving finite volume schemes for hyperbolic heat equation on unstructured meshes. Numerische Mathematik, Volume 122, Issue 2, pp 227-278 (2012).
14. C. Chalons, F. Coquel, E. Godlewski, P.-A. Raviart, and N. Seguin. Godunov-type schemes for hyperbolic systems with parameter-dependent source. The case of Euler system with friction. Math. Models Methods Appl. Sci. 20 (2010), no. 11, 21092166. MR 2740716 (2011m:65179).
15. S. Chapman. Phil. Trans. Roy. Soc. London 216 (1916) 279.
16. S. Chapman and T. G. Cowling. The Mathematical Theory of Non-Uniform Gases. Cambridge University Press, Cambridge, England, 1995.
17. P. Charrier, B. Dubroca, G. Duffa, and R. Turpault. Multigroup model for radiating flows during atmospheric hypersonic re-entry. Proceedings of International Workshop on Radiation of High Temperature Gases in Atmospheric Entry, pp. 103110. Lisbonne, Portugal. (2003).
18. F. Chen. *Introduction to Plasma Physics and Controlled Fusion, (1984)*. Plenum Press, New York.
19. G Dimarco and L Pareschi. Asymptotic Preserving Implicit-Explicit Runge–Kutta Methods for Nonlinear Kinetic Equations. SIAM Journal on Numerical Analysis 51 (2013), 1064-1087.
20. J.F. Drake, P.K. Kaw, Y.C. Lee, G. Schmidt, C.S. Liu, and M.N. Rosenbluth. Parametric instabilities of electromagnetic waves in plasmas. Phys. Fluids 17, 778, 1974.
21. B. Dubroca, J.-L. Feugeas, and M. Frank. Angular moment model for the Fokker-Planck equation. European Phys. Journal D, 60, 301, (2010).
22. B. Dubroca and J.L. Feugeas. Entropic moment closure hierarchy for the radiative transfert equation. C. R. Acad. Sci. Paris Ser. I, 329 915, (1999).
23. B. Dubroca and J.L. Feugeas. Étude théorique et numérique d'une hiéarchie de modèles aux moments pour le transfert radiatif. C. R. Acad. Sci. Paris, t. 329, SCrie I, p. 915-920, (1999).
24. R. Duclous, B. Dubroca, F. Filbet, and V. Tikhonchuk. High order resolution of the Maxwell-Fokker-Planck-Landau model intended for ICF applications. J. Comput. Phys. 228(14): 5072-5100 (2009).
25. D. Enskog. Kinetische Theorie der Vorgnge in Mssig Verdnnten Gasen. Uppsala, 1917.
26. E. Epperlein and R. Short. Phys. Fluids B 4, 2211 1992.
27. F. Filbet and S. Jin. A class of asymptotic preserving schemes for kinetic equations and related problems with stiff sources. J. Comp. Phys. vol. 229, no 20 (2010).
28. L. Gosse and G. Toscani. Space localizaion and well-balanced schemes for discrete kinetic models in diffusive regimes. SIAM J. Numer. Anal. 41 (2) (2003) 641658.

29. H. Grad. On the kinetic theory of rarefied gases. Commun. Pure Appl. Math. 2, 331-407 (1949).
30. C.P.T. Groth and J.G. McDonald. Towards physically-realizable and hyperbolic moment closures for kinetic theory. Continuum Mech. Thermodyn. 21, 467-493 (2009).
31. S. Guisset, S. Brull, E. d'Humières, and B. Dubroca. Asymptotic-preserving well-balanced scheme for the electronic M_1 model in the diffusive limit: particular cases. Submitted, hal-01145044.
32. S. Guisset, S. Brull, B. Dubroca, E. d'Humières, S. Karpov, and I. Potapenko. Asymptotic-preserving scheme for the Fokker-Planck-Landau-Maxwell system in the quasi-neutral regime. Communications in Computational Physics, volume 19, issue 02, pp. 301-328 (2016).
33. S. Guisset, S. Brull, E. dHumires, B. Dubroca, and V. Tikhonchuk. Classical transport theory for the collisional electronic M1 model. Physica A: Statistical Mechanics and its Applications, Volume 446, Pages 182-194 (2016).
34. S. Guisset, J.G. Moreau, R. Nuter, S. Brull, E. dHumières, B. Dubroca, and V.T. Tikhonchuk. Limits of the M1 and M2 angular moments models for kinetic plasma physics studies. J. Phys. A: Math. Theor. 48, 335501 (2015).
35. A. Harten, P.D. Lax, and B. Van Leer. On upstream differencing and Godunov-type schemes for hyperbolic conservation laws. SIAM Review 25 (1983), 35-61.
36. S. Jin and C.D. Levermore. Fully discrete numerical transfer in diffusive regimes. Transport Theory Statist. Phys. 22 (6) 739791. (1993).
37. S. Jin and C.D. Levermore. The discrete-ordinate method in diffusive regimes. Transport Theory Statist. Phys. 20 (56) 413439. (1991).
38. P. Lafitte and G. Samaey. Asymptotic-preserving projective integration schemes for kinetic equations in the diffusion limit. SIAM Journal on Scientific Computing , 34(2):A579 A602, 2012.
39. L. Landau. On the vibration of the electronic plasma. J. Phys. USSR 10 (1946).
40. M. Lemou and L. Mieussens. A New Asymptotic Preserving Scheme Based on Micro-Macro Formulation for Linear Kinetic Equations in the Diffusion Limit. SIAM J. Sci. Comput., 31(1), 334368, 2008.
41. C.D. Levermore. Moment closure hierarchies for kinetic theories. J. Stat. Phys. 83, 1021-1065 (1996).
42. J. Mallet, S. Brull, and B. Dubroca. An entropic scheme for an angular moment model for the classical Fokker-Planck-Landeau equation of electrons. Comm. Comput. Phys., 422, (2013).
43. J. Mallet, S. Brull, and B. Dubroca. General moment system for plasma physics based on minimum entropy principle. Kinetic and Related Models, vol. 8, No.3, 533-558, (2015).
44. A. Marocchino, M. Tzoufras, S. Atzeni, A. Schiavi, Ph. D. Nicola, J. Mallet, V. Tikhonchuk, and J.-L. Feugeas. Nonlocal heat wave propagation due to skin layer plasma heating by short laser pulses. Phys. Plasmas 20, 022702, (2013).
45. J.G. McDonald and C.P.T. Groth. Towards realizable hyperbolic moment closures for viscous heat-conducting gas flows based on a maximum-entropy distribution. Continuum Mech. Thermodyn. 25, 573-603 (2012).
46. N. Meezan, L. Divol, M. Marinak, G. Kerbel, L. Suter, R. Stevenson, G. Slark, and K. Oades. Phys. Plasmas 11, 5573 2004.
47. G.N. Minerbo. Maximum entropy Eddigton Factors. J. Quant. Spectrosc. Radiat. Transfer, 20, 541, (1978).
48. I. Muller and T. Ruggeri. Rational Extended Thermodynamics. Springer, New York (1998).
49. Ph. D. Nicola, J.-L. A. Feugeas, and G. P. Schurtz. A practical nonlocal model for heat transport in magnetized laser plasmas. Phys. Plasmas 13, 032701, (2006).
50. J.-F. Ripoll. An averaged formulation of the M1 radiation model with presumed probability density function for turbulent flows. J. Quant. Spectrosc. Radiat. Trans. 83 (34), 493517. (2004).
51. W. Rozmus, V. T. Tikhonchuk, and R. Cauble. A model of ultrashort laser pulse absorption in solid targets. Phys. Plasmas 3, 360 (1996).

52. S.Boscarino, P.G. LeFloch, and G. Russo. High-order asymptotic-preserving methods for fully nonlinear relaxation problems. SIAM J. Sci. Comput. Vol. 36, No.2, pp.A377-A395.
53. K. Shigemori, H. Azechi, M. Nakai, M. Honda, K. Meguro, N. Miyanaga, H. Takabe, and K. Mima. Phys. Rev. Lett. 78, 250 1997.
54. I.P. Shkarofsky, T.W. Johnston, and The Particle Kinetics of Plasmas M.P. Bachynski. Addison-Wesley (Reading, Massachusetts, 1966).
55. L. Spitzer and R. Härm. Phys. Rev. 89 (1953) 977.
56. H. Struchtrup. Macroscopic Transport Equations for Rarefied Gas Flows. Springer, Berlin (2005).
57. R. Turpault. A consistent multigroup model for radiative transfer and its underlying mean opacity. J. Quant. Spectrosc. Radiat. Transfer 94, 357371 (2005).
58. R. Turpault, M. Frank, B. Dubroca, and A. Klar. Multigroup half space moment approximations to the radiative heat transfer equations. J. Comput. Phys. 198 363 (2004).
59. A. Velikovich, J. Dahlburg, J. Gardner, and R. Taylor. Phys. Plasmas 5, 1491 1998.